PHILOSOPHICAL TRANSACTIONS OF THE ROYAL SOCIETY A

rsta.royalsocietypublishing.org

Research

Cite this article: Milne IA, Sharma RN, Flay RGJ, Bickerton S. 2013 Characteristics of the turbulence in the flow at a tidal stream power site. Phil Trans R Soc A 371: 20120196. http://dx.doi.org/10.1098/rsta.2012.0196

One contribution of 14 to a Theme Issue 'New research in tidal current energy'.

Subject Areas:
mechanical engineering, ocean engineering

Keywords:
acoustic Doppler velocimetry, turbulence, turbulence intensity, turbulence spectrum, integral scales, tidal stream power

Author for correspondence:
I. A. Milne
e-mail: imil015@aucklanduni.ac.nz

Characteristics of the turbulence in the flow at a tidal stream power site

I. A. Milne, R. N. Sharma, R. G. J. Flay and S. Bickerton

Department of Mechanical Engineering, The University of Auckland, Auckland 1142, New Zealand

This paper analyses a set of velocity time histories which were obtained at a fixed point in the bottom boundary layer of a tidal stream, 5 m from the seabed, and where the mean flow reached 2.5 m s^{-1}. Considering two complete tidal cycles near spring tide, the streamwise turbulence intensity during non-slack flow was found to be approximately 12–13%, varying slightly between flood and ebb tides. The ratio of the streamwise turbulence intensity to that of the transverse and vertical intensities is typically 1 : 0.75 : 0.56, respectively. Velocity autospectra computed near maximum flood tidal flow conditions exhibit an $f^{-2/3}$ inertial subrange and conform reasonably well to atmospheric turbulence spectral models. Local isotropy is observed between the streamwise and transverse spectra at reduced frequencies of $f > 0.5$. The streamwise integral time scales and length scales of turbulence at maximum flow are approximately 6 s and 11–14 m, respectively, and exhibit a relatively large degree of scatter. They are also typically much greater in magnitude than the transverse and vertical components. The findings are intended to increase the levels of confidence within the tidal energy industry of the characteristics of the higher frequency components of the onset flow, and subsequently lead to more realistic performance and loading predictions.

1. Introduction

In recent years, the tidal stream energy industry has witnessed significant growth, with numerous commercial-scale schemes now in development globally. However, a number of early generation turbines have failed prematurely, owing, in part, to the harsh operating environment to which they are exposed. While the characteristics of the mean flow at tidal energy sites are

Royal Society Publishing
Informing the science of the future

relatively well understood and simple to measure, a lack of confidence in the characteristics of the turbulent flow has subsequently resulted in high levels of conservativeness being employed by turbine designers [1]. This must be addressed if tidal stream power is to become more commercially competitive with other forms of electricity generation.

This paper reports on the analysis of relatively high-frequency (4 Hz) instantaneous velocity measurements obtained at a proposed tidal energy site, where during spring tide the mean flow in the bottom boundary layer is of the order of $2\,\mathrm{m\,s^{-1}}$. The objectives of the study were to examine the intensity of the turbulent velocity fluctuations, as well as to characterize the spectral nature of the turbulent energy. It is envisaged that developers of tidal stream turbines can use the findings to assist them in obtaining more accurate performance and loading predictions.

Recently, there have been published reports of attempts to quantify the structure of the flow at tidal energy sites using acoustic Doppler current profilers (ADCPs) [2,3], in which the velocity at different points through the water column can be measured co-currently. While four-beam ADCPs can be readily used to obtain the variation in the mean flow in the bottom boundary layer, the non-homogeneous nature of the flow, coupled with the horizontal spreading of the ADCP beams, imposes a restriction on the length scales of the instantaneous velocities which can be studied accurately. These scales can be of the order of a typical rotor diameter.

Point measurement techniques are, therefore, arguably more suitable for analysing the higher frequency instantaneous velocity components. However, relevant literature is limited to flows typically lower than what would be necessary for tidal power generation. Early field measurements published by Grant *et al.* [4] involved the use of a hot-film flow meter to measure the streamwise velocity fluctuations, and for which an inertial and dissipation subrange was observed in the computed spectra. Heathershaw [5] and Bowden and co-workers [6–9] have previously used electronic current meters to measure the horizontal and vertical velocity fluctuations in the bottom boundary layer of a tidal channel, at distances of up to 2 and 1.75 m from the seabed, respectively, where the mean flow speed was of the order of $0.5–1\,\mathrm{m\,s^{-1}}$. The velocity spectra exhibited similarities to those of atmospheric boundary layer turbulence, although Heathershaw [5] discusses that the agreement is typically closer for relatively narrow tidal channels.

More recently, point measurements of instantaneous velocities have been obtained using acoustic Doppler velocimeters (ADVs), in which the three-dimensional velocities of a small sampling volume can be inferred from acoustic receivers using the Doppler shift principle. The use and accuracy of ADVs for measuring turbulence in flumes and in the field have been reported [10–12]. More recently, Thomson *et al.* [13] have compared the ADV and ADCP velocity time histories from a tidal channel in Puget Sound, WA, and demonstrated good agreement between the turbulence intensities once Doppler noise in the ADCP had been corrected for. However, additional literature on the application of ADVs for measuring the instantaneous velocities in relatively fast-flowing tidal streams is scarce. One contributing factor is the inherent difficulty in obtaining accurate measurements in such flows because of sensor movement and vibration, and, for fixed sensors, the effect on the flow by the structure to which the sensor is attached.

2. Deployment location and experimental set-up

The velocity measurements analysed in this study were obtained at the Sound of Islay, UK, at a location of 55 50.432′ N, 006 05.900′ W, shown in figure 1. The site is currently being developed by ScottishPower Renewables (http://www.scottishpowerrenewables.com) together with tidal turbine manufacturer Andritz Hydro Hammerfest (http://www.hammerfeststrom.com), which have proposed the installation of 10 generating devices each rated at 1 MW. The site is considered favourable for tidal stream energy generation, as it has relatively strong currents and is sheltered from large surface waves.

The measurements were conducted in the bottom boundary layer at a distance of 5 m from the seabed, and the mean water depth is 55 m. The sensor was attached rigidly to a steel

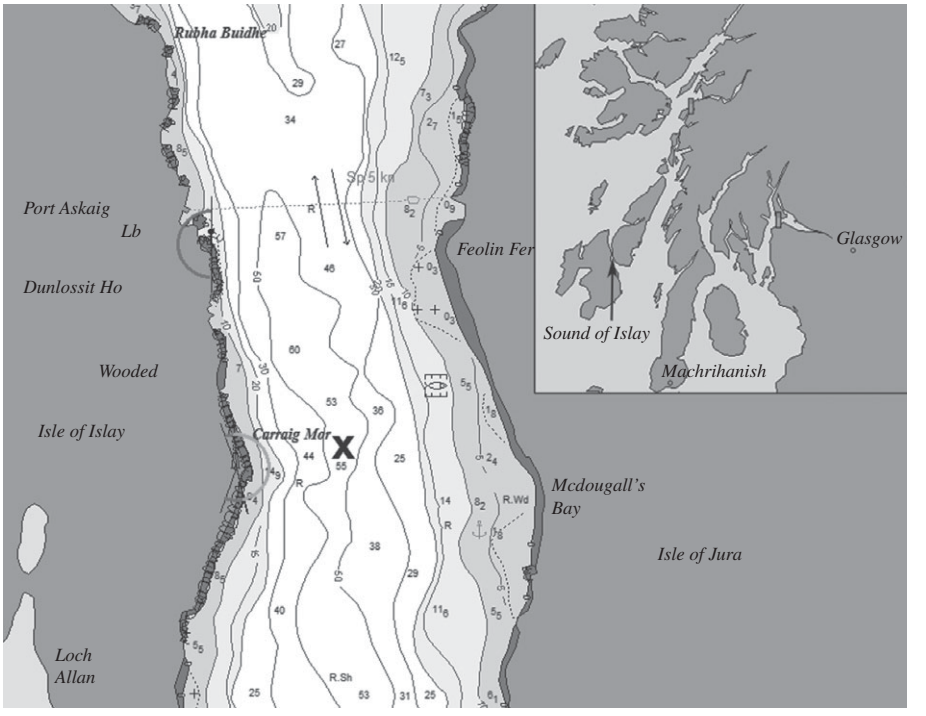

Figure 1. Map of the Sound of Islay, aligned north, with depth contours (metres) and the ADV deployment location indicated by 'X'. The location of the Sound of Islay in the Inner Hebrides of Scotland, UK, is shown top right. Adapted from Admiralty Charts acquired from the UK Hydrographic Office (http://www.ukho.gov.uk).

frame, as can be observed in figure 2, which was submerged and located on the seabed for the duration of the data acquisition. A tri-beam Nortek Vector ADV (http://www.nortekusa.com/en/products/velocimeters/vector), aligned vertically with the probe above the canister, was used to measure the three components of velocity. It was operated in continuous mode with a sampling frequency of 4 Hz over a period of approximately 15 days, encompassing both a spring and neap tidal cycle. The orientation of the sensor (heading, pitch and roll) was measured simultaneously, with a sampling frequency of 1 Hz.

3. Data processing

Prior to analysis, a quality assurance check of the raw data was undertaken. While the motion of the frame was relatively minor and was observed to typically be greatest during acceleration of the current, samples where excessive compass motion was present were removed. These samples were identified as having a heading, pitch or roll angle standard deviation in excess of 0.2°, and totalled 4 per cent of all the samples considered. For the remaining samples, instantaneous velocity signals corresponding to signal-to-noise ratios of less than 15 dB and correlations of less than 70 per cent were replaced as recommended by the sensor manufacturer [14]. The beam velocities were then transformed to an Earth-fixed reference frame, with the horizontal velocities then resolved into streamwise (in the direction of the mean flow) and transverse components using the mean flow directions from the entire deployment period. Spikes in the high-pass filtered individual velocity components were detected using the phase-space threshold technique proposed by Goring & Nikora [12], and replaced with cubically interpolated data either side of the spike. The effect of removing errors and despiking is demonstrated in figure 3 for a 60 s extract from a typical sample velocity history. In general, however, the raw velocities used for analysing

Figure 2. The frame as used in experiments with the ADV rigidly mounted to the top of the mast, prior to deployment onto the seabed for the duration of the data acquisition period. Photo supplied courtesy of Partrac Ltd, Glasgow, UK (http://www.partrac.com).

turbulent statistics were considered to be of high quality. Excluding samples with excessive data motion, the instantaneous data points replaced were 5.8 per cent of the total (172 800) data points analysed in this study, nearly all (5.4%) owing to despiking. The resulting effect on the standard deviation of all the samples was negligible, with the median difference being 0.6 per cent, 1.5 per cent and 2.5 per cent in the streamwise, transverse and vertical components, respectively.

The velocities were analysed (and despiked) using a sample duration of 5 min (1200 data points), computed every minute and which, therefore, overlapped. The time period of the samples was deemed to provide an appropriate resolution from which to study the dominant turbulence scales. A test for stationarity was conducted using the non-parametric 'runs test' described by Bendat & Piersol [15], and where an average of 94 per cent of the total samples were deemed to be stationary. The number of stationary samples decreased for lower velocities, which can probably be attributed to a higher flow acceleration. All samples were detrended using a linear least-squares regression technique.

4. Mean flow characterization

The 5 min time-averaged East and North velocities provide an initial basis from which to establish the underlying nature of the flow. Their variation over the entire deployment period is shown in figure 4. The mean flow exhibits a high degree of bi-directionality, as would be expected given the relatively narrow passage of water at the Sound of Islay. The mean heading is 343° from North at flood and 158° at ebb, respectively. At spring and neap tide the maximum velocities are approximately 2.5 and 1.2 m s^{-1}, respectively.

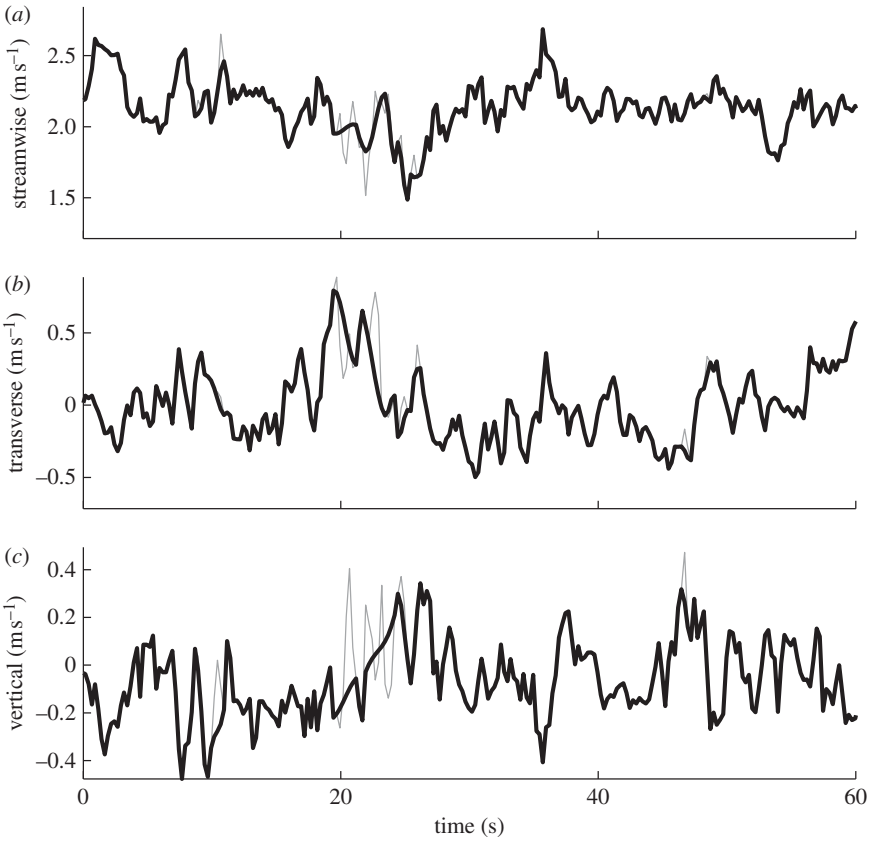

Figure 3. A 60 s extract from a typical time history where $U \approx 2.0$ m s^{-1}, depicting the identification and replacement of data where the signal-to-noise ratio or correlation is too low, or where an erroneous spike is present. Raw velocities are shown in grey and processed velocities are shown in black.

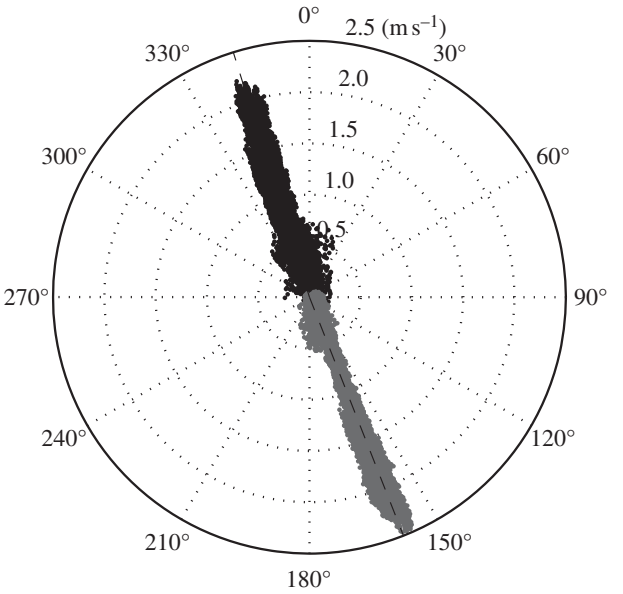

Figure 4. The mean flow velocity magnitude and compass direction of 20 248, 5 min samples obtained every 1 min over the entire measurement period at a distance of 5m above the seabed, for both ebb and flood tides.

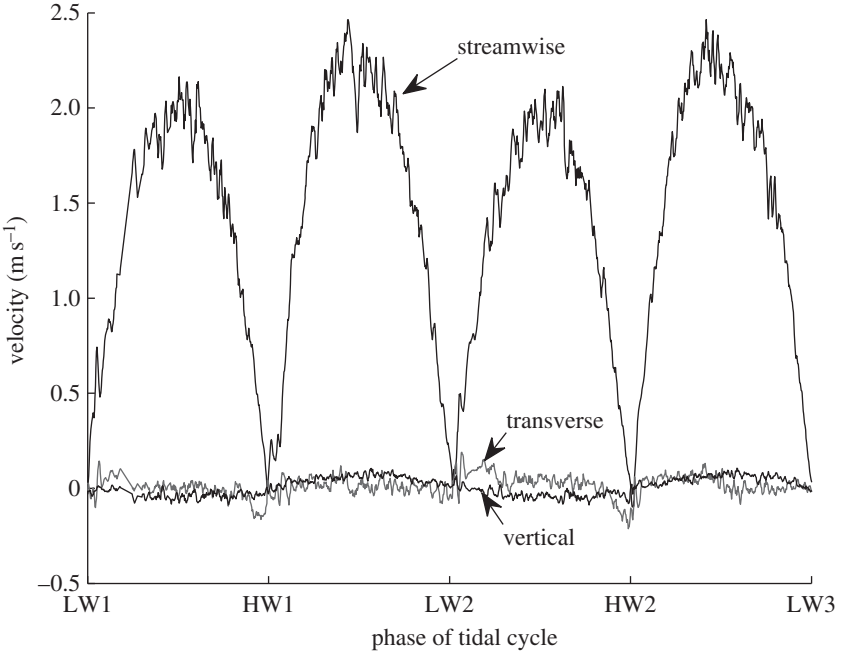

Figure 5. The median-averaged streamwise, transverse and vertical velocity time histories at a distance of 5 m above the seabed, computed from 5 min samples obtained every 1 min over two tidal cycles near spring tide. LW and HW denote low water and high water, respectively.

In this study, the higher velocity components are analysed over the duration of two consecutive tidal cycles near spring tide. The time histories of the time-averaged mean velocities over these cycles are shown in figure 5. The maximum velocity magnitude is shown to be greater at ebb tide than during the flood by approximately $0.5\,\mathrm{m\,s^{-1}}$, but there appears to be little variability between consecutive ebb or flood tides. The transverse and vertical velocities are comparatively of much smaller magnitude. The vertical velocity can be observed to exhibit an underlying harmonic variation, which is in-phase with the streamwise velocity. It is postulated that this is likely to be due to bias in the measurement of the compass directions, which results in components of true horizontal velocities being resolved into the vertical direction. However, the wake from the structure and sensor, as discussed by Trevethan [16], or the topography of the seabed, may also induce a vertical flow.

5. Turbulence characterization

(a) Turbulence intensities

The higher frequency velocity characteristics are first analysed in terms of the turbulence intensity $I_i(=\sigma_i/U)$, defined as the ratio of the standard deviation, σ_i, of the streamwise, transverse and vertical velocity fluctuation components ($i=u,v,w$) to the mean streamwise velocity of each sample. This parameter provides a quantification of the magnitude of the turbulent fluctuations and is considered to be a dominant driver of the fatigue loads on tidal turbine blades [17].

The streamwise turbulence intensity time history, computed from the 5 min long samples, is shown in figure 6*a*. It is shown to be relatively constant during the majority of the tidal cycle, at approximately 13 per cent at flood and 12 per cent during ebb. These values generally agree favourably with those presented in the literature. Osalusi [2] has presented estimates of a parameter related to the turbulent kinetic energy density ($q^2/2=(\sigma_u^2+\sigma_v^2+\sigma_w^2)/2$) from ADCP measurements at the Fall of Warness, UK, for which the anisotropic ratios used by

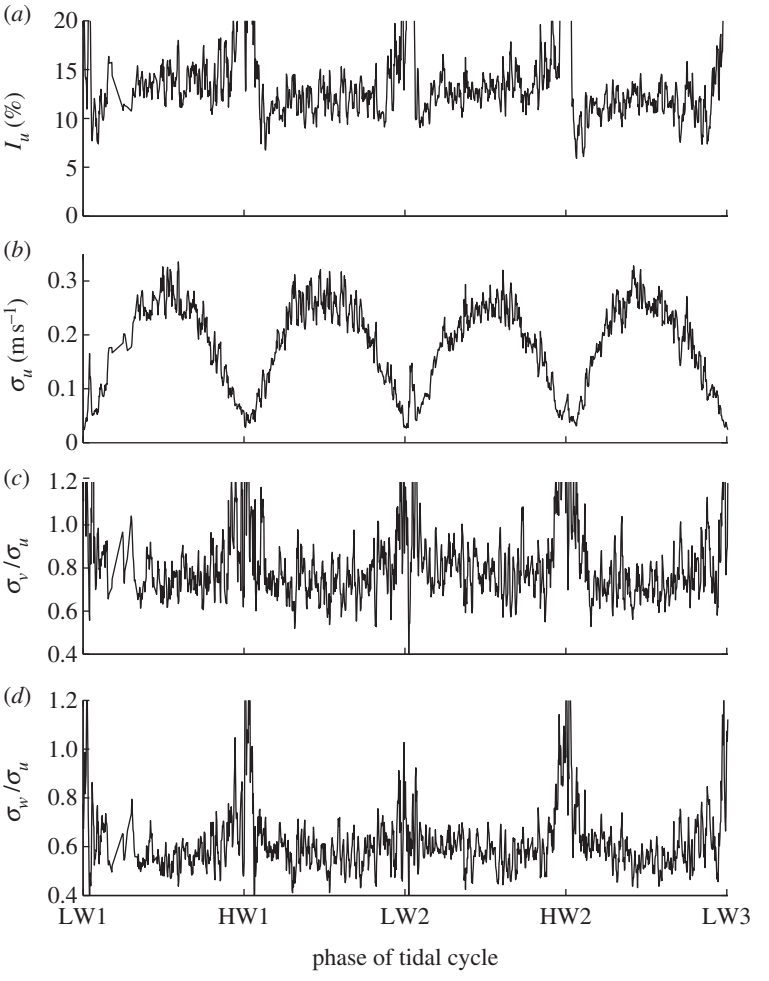

Figure 6. Time histories over the tidal cycle of: (*a*) the turbulence intensity and (*b*) the standard deviation of the streamwise fluctuating velocity; and ratios of the (*c*) transverse and (*d*) vertical standard deviations to that of the streamwise component. The parameters have been computed from 5 min samples obtained every 1 min. An upper limit has been imposed on the parameters shown, which become excessive at slack water.

Stacey *et al.* [18] are assumed. At 5 m above the seabed, where the mean flow reached 1.5 m s^{-1}, these correspond to streamwise turbulence intensities ranging between 10 and 11 per cent. The streamwise turbulence intensity, measured 4.6 m above the seabed at Puget Sound by Thomson *et al.* [13], was found to be similar, at approximately 10–11%. Li *et al.* [3] have also reported on turbulence intensities computed from ADCP measurements in the East River, New York, NY, where the water depth was comparatively shallow, varying between 7 and 9 m. They found, however, that the streamwise turbulence intensity 5 m above the seabed in $U \approx 2$ m s^{-1} flows was of the order of 25–30%. This suggests that the turbulence intensity may be somewhat site specific. The time history of the standard deviation of the streamwise velocity fluctuations is shown in figure 6*b*, and varies in phase with the tidal cycle. The standard deviation is approximately 0.27 m s^{-1} during both peak flood and ebb flow, and can exceed 0.30 m s^{-1}. This implies that the difference observed between the magnitudes of the flood and ebb turbulence intensity is likely to be due to the aforementioned difference in magnitude of the flood and ebb mean velocity.

The ratios of standard deviation (or turbulence intensity) of the transverse and vertical fluctuating velocity to that of the streamwise component are shown in figure 6*c*,*d*, respectively. During peak flood and ebb flow, the ratios can be observed to be approximately $\sigma_u : \sigma_v : \sigma_w =$

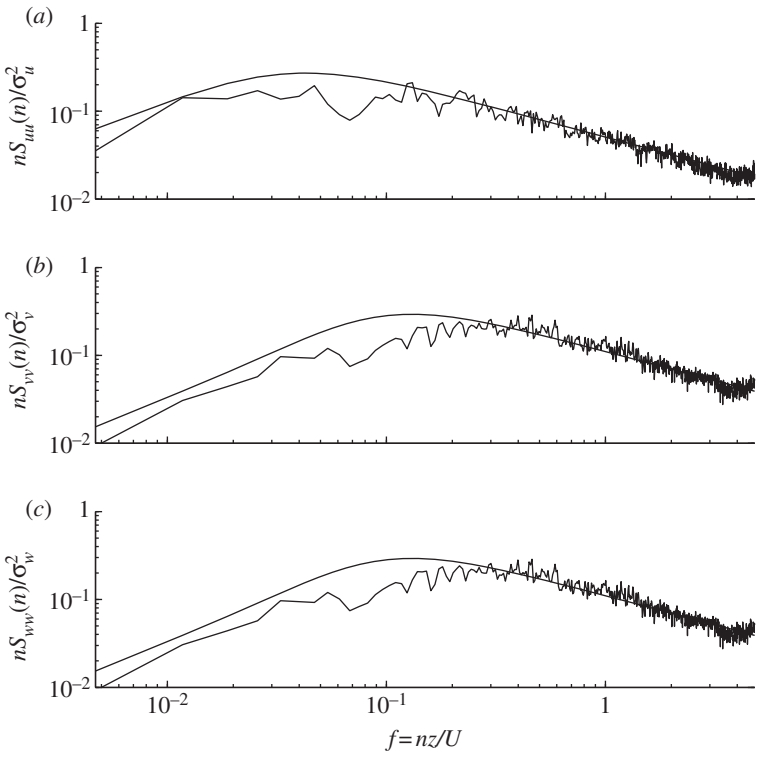

Figure 7. Normalized autospectra of measured velocity fluctuations, and empirical predictions from the von Kármán model, plotted against reduced frequency, averaged from 119, 5 min samples obtained every 1 min 15° either side of the phase in which maximum flood tide occurs. Median velocity ($U = 2\ \mathrm{m\ s^{-1}}$).

1 : 0.75 : 0.56. Nezu & Nakagawa [19] suggest the ratios are $\sigma_u : \sigma_v : \sigma_w = 1 : 0.71 : 0.55$ for two-dimensional open channel flows, as inferred from experiments at relatively low Reynolds numbers ($Re \approx 10^4$). These ratios agree well with the measured ratios, especially given the differences between such an idealized case and that at the Sound of Islay, in terms of bathymetry and the Reynolds number, the latter of which is several orders of magnitude greater. In terms of the atmospheric turbulent boundary layer, the ratios of $\sigma_u : \sigma_v : \sigma_w = 1 : 0.68 : 0.45$ are suggested in the study of Cook [20], which are lower than those measured here, and are perhaps due to them not being based on two-dimensional flow.

(b) Velocity spectra

The turbulence intensity of the velocity functions, however, provides little insight into the structure of the flow. Velocity autospectra have therefore been computed that can assist in inferring the stochastic distribution of turbulent energy. The spectra analysed here are from samples 15° either side of the phase in which the maximum flood velocity occurs. Referring to figure 5, the mean velocity of each sample is approximately $U \approx 2\ \mathrm{m\ s^{-1}}$. A frequency averaging technique was applied to smooth the spectra.

The autospectra of each of the three velocity fluctuation components are shown in figure 7, in terms of the normalized spectral density and against a normalized frequency $f(=nz/U)$ on the abscissa, where n is the frequency in Hz and z is the distance above the seabed in metres. The spectra exhibit the form typical of boundary layer turbulence, with an inertial subrange proportional to $f^{-2/3}$ observed at the high-frequency tail. There appears to be no dominant spectral frequency component within the inertial subrange. The peaks of the spectra, which are typically indicative of the scales corresponding to the large energy-producing eddies, are

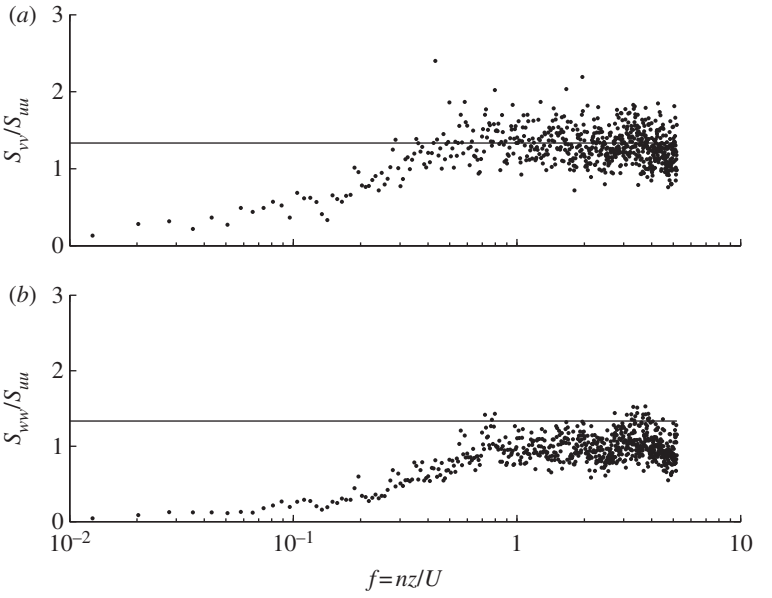

Figure 8. Ratio of the transverse and vertical spectral densities to that of the streamwise component, for 119, 5 min samples obtained every 1 min 15° either side of the phase in which maximum flood tide occurs. Median velocity ($U = 2\,\mathrm{m\,s^{-1}}$). The ($\frac{4}{3}$) ratio is indicated by a solid line.

at considerably higher frequencies for the transverse and vertical components, relative to the spectrum of the streamwise component. This suggests that there is a significant degree of anisotropy in the large scales. At very high frequencies, $f \approx 4$, the spectra can be observed to flatten, which is indicative of the influence of Doppler noise and aliasing effects. However, since this region is relatively small, no attempts have been made to adjust the spectra.

The analysis also provides the opportunity to assess the applicability of empirical models commonly employed to model atmospheric boundary layer turbulence. In this study, the von Kármán empirical turbulence model [21] is used for comparison, for which the normalized spectral density function is expressed as

$$\frac{nS_{uu}}{\sigma_u^2} = \frac{4\tilde{\eta}_u}{(1+70.8\tilde{\eta}_u^2)^{5/6}}, \tag{5.1}$$

for the streamwise component, where $\tilde{\eta}_u (= nL_u/U)$ is a non-dimensional frequency, and

$$\frac{nS_{ii}}{\sigma_i^2} = \frac{4\tilde{\eta}_i(1+755.2\tilde{\eta}_i^2)}{(1+282.3\tilde{\eta}_i^2)^{11/6}}, \tag{5.2}$$

for the transverse and vertical components, where $i = v, w$.

The von Kármán autospectra are superimposed on the individual spectra in figure 7, which have been computed for integral length scales $L_u = 17\,\mathrm{m}$, $L_v = 4\,\mathrm{m}$ and $L_w = 4\,\mathrm{m}$. Relatively good agreement with the relative positions of the spectral peak and inertial subrange can be observed between the measured and modelled spectra. This suggests that the von Kármán model could feasibly allow for a relatively realistic representation of the bottom boundary layer for this particular tidal flow.

While the low-frequency scales exhibit anisotropy, isotropy should theoretically be observed within the inertial subrange. Under isotropic conditions, the spectral densities of the transverse and vertical fluctuating velocities, $S_{vv}(n)$ and $S_{ww}(n)$, are expected to be equal to $(\frac{4}{3})S_{uu}(n)$, which provides a useful test for the inception of local isotropy. The spectral density ratios computed from the measured velocities are shown in figure 8, where the ratio for the transverse component can

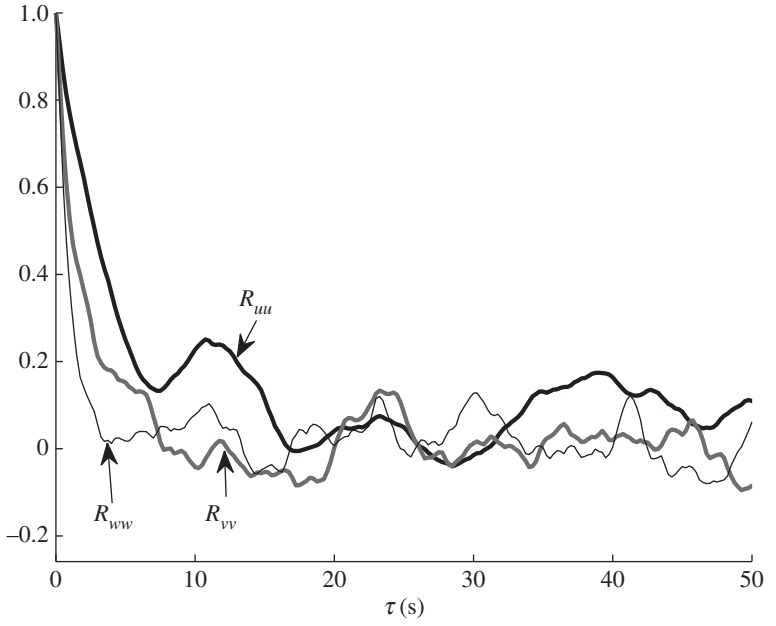

Figure 9. An example of the autocorrelation function for the three components of velocity, for a sample where the mean velocity $U = 2.0\ \mathrm{m\,s^{-1}}$. The integral time scales are computed by integrating the autocorrelation function from $\tau = 0$ to the first instance of $R_{ii} = 0$. For this case, $T_u = 6.2$ s, $T_v = 1.9$ s and $T_w = 1.6$ s.

be observed to approach $(\frac{4}{3})$ for reduced frequencies $f > 0.5$. The ratio of the horizontal to vertical components appears to tend towards a smaller value of approximately 1, for reduced frequencies $f > 0.8$. A $S_{ww}(n) = (\frac{4}{3})S_{uu}(n)$ ratio was observed by Lien & Sanford [22] in an unstratified tidal channel. This difference is likely to be due to the horizontal velocity components being affected by noise to a greater extent than the vertical component. Other factors such as the local topography of the seabed or vortex shedding off the supporting frame structure may also have an influence.

(c) Integral scales of turbulence

The degree of anisotropy in the flow has been further investigated by considering the variation in time of the integral time scales of turbulence. The integral time scales are a measure of the duration for which the largest eddies remain correlated. In this study, the scales are computed for each sample from

$$T_i = \int_{\tau=0}^{\tau(R_{ii}(\tau)=0)} R_{ii}(\tau)\,\mathrm{d}\tau, \tag{5.3}$$

where $R_{ii}(\tau)$ is the autocorrelation function. In the streamwise direction, the autocorrelation function is expressed as

$$R_{uu}(\tau) = \frac{R(u(t), u(t+\tau))}{\sigma_u^2}, \tag{5.4}$$

where u is the fluctuating streamwise velocity component. The autocorrelation function is integrated with respect to time between the limits $\tau = 0$ and the first instance of $R_{ii} = 0$. An example of the autocorrelation, for a sample where the mean velocity $U = 2.0\ \mathrm{m\,s^{-1}}$, is shown in figure 9. The autocorrelation can be observed to decay as the time lag increases and also exhibits a degree of periodicity due to large low-frequency oscillations in the flow.

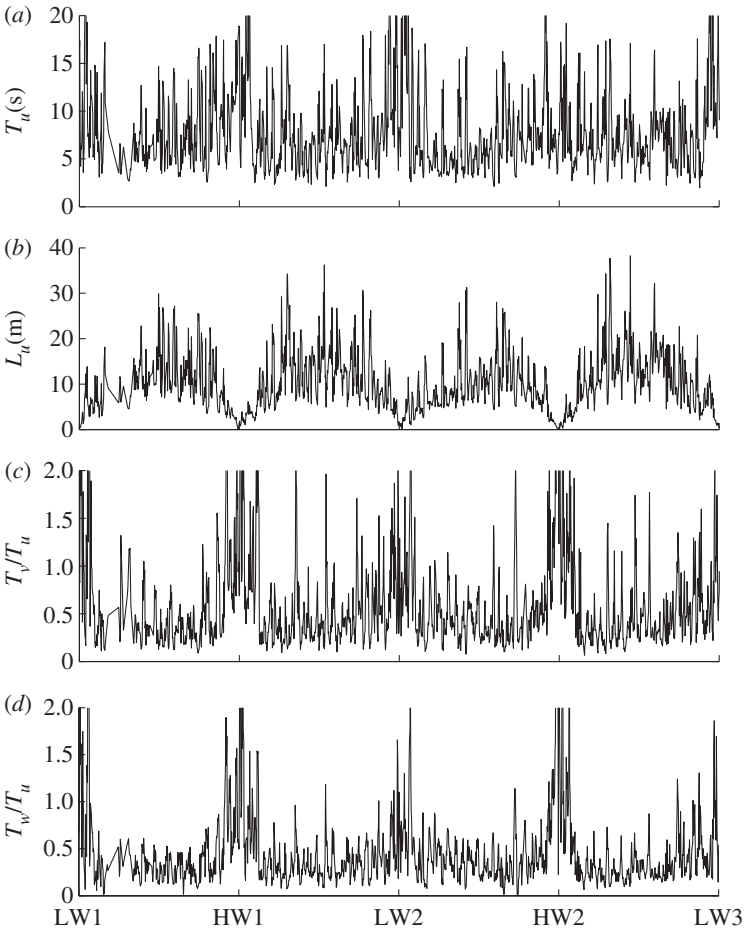

Figure 10. Time histories over the tidal cycle of: (*a*) the integral time scales and (*b*) length scales of the streamwise turbulence component; and ratios of the integral time scales of the (*c*) transverse and (*d*) vertical standard turbulence component to that of the streamwise component, computed from 5 min samples obtained every 1 min.

The variation of the streamwise integral time scale over the tidal cycle is shown in figure 10*a*. The median streamwise time scales computed from samples within 15° of maximum flood and ebb tide are 5.7 s and 6.0 s, respectively. The integral length scales of turbulence are also shown in figure 10*b*, which have been estimated by invoking Taylor's frozen turbulence hypothesis $L_i = UT_i$. The integral length scales corresponding to the aforementioned time scales are approximately 11.3 m during flood tide and 13.6 m during ebb tide.

Time averages over the tidal cycle of the ratio of the transverse and vertical integral time scales to that for the streamwise scale are shown in figure 10*c*,*d*, respectively. The ratios appear to be relatively similar, tending towards a value of approximately $0.2T_u$. These ratios are approximately equal to those which were employed in the von Kármán model previously. It can also be observed that the degree of scatter is comparatively smaller in the transverse and vertical scales than in the streamwise scales.

In terms of comparisons with open channel flow theory, Nezu & Nakagawa [19] suggest that in two-dimensional flow in the lower half of the water column the streamwise integral scales conform to the relationship

$$L_u \approx \sqrt{zh}, \tag{5.5}$$

where h is the channel depth and z is the distance from the seabed.

Assuming such a relationship, an integral length scale of 16 m and a time scale of 8 s would be expected for this study. This agrees relatively well with the scales computed in the present measurements, supporting a scaling with channel depth and distance from the seabed. This is despite the Reynolds numbers in the present study being several orders of magnitude greater than those for the experiments ($Re \approx 10^4$) from which equation (5.5) was developed.

6. Discussion

The unsteady performance and loads of a tidal turbine are typically analysed within the industry by using a synthesized velocity field. Often, atmospheric empirical spectral models have been employed in lieu of such a model for turbulence in a high-velocity tidal stream. The velocity spectra computed in this study suggest that an atmospheric spectral model is likely to enable a reasonably accurate representation of the turbulence, notably in the inertial subrange.

Obtaining the integral scales of turbulence, which are required to compute the spectral density, may be difficult, however, owing to their relatively large fluctuations and sensitivity to low frequencies. However, the findings appear to suggest that they are functions of the channel geometry and distance from the seabed. It is also important to consider that the level of agreement observed between the atmospheric and measured velocity spectra may be due to the tidal channel at the Sound of Islay being relatively narrow, and, as Heathershaw [5] discusses, it is possible that the agreement could be reduced for wider flows where there are potentially larger transverse scales of motion. Also this study only considered the spectra at maximum velocity, during near spring tide, and at one height point above the seabed. Any differences that may exist between slower flows, over a spring–neap tidal cycle, or through the water column have not been considered.

Whether or not an accurate estimate of the integral time scale is necessary can be argued. A parametric assessment of the sensitivity of the fatigue loads of tidal turbine blades by Milne *et al.* [17] indicated that the integral length scales have a much smaller role than the turbulence intensity. The variations in the turbulence intensity of the velocity are shown here to be relatively low, and one would expect to be able to obtain an estimate of the turbulence intensity with a good degree of confidence.

While point measurements permit the instantaneous velocities to be analysed at relatively high frequencies, it should also be appreciated that the transverse and vertical spatial variation of the streamwise velocity cannot be measured. The spectral characteristics of the freestream velocity incident on a rotating turbine blade differ from those for a fixed point. Large eddies, non-coherent across the rotor plane, can be encountered multiple times by a rotating blade. This results in an effective increase in spectral energy at multiples of the rotational frequency, and a decrease in energy at the frequencies in between, relative to the fixed point spectrum.

Connell [23] has derived an analytical expression for the turbulent velocity spectrum for a point on a rotating blade from the von Kármán turbulence spectrum and corresponding coherence functions. The model was employed in Milne *et al.* [17] to explore the implications of rotational sampled turbulence on a typical tidal turbine. Obtaining high-frequency point measurements over a sufficiently wide area, which would enable the spatial coherence to be measured and the model to be verified, is inherently challenging in a fast-flowing tidal stream. One would expect however, given the relatively good agreement that was observed between the measured and the von Kármán spectra, that the analytical form of the rotational sampled spectrum in the study of Connell [23] would permit sensible predictions of the dominant frequencies.

7. Conclusions

The objective of this study was to gain an understanding of the turbulence characteristics in the bottom boundary layer of the tidal stream at the Sound of Islay, where the maximum flow velocity is approximately 2 m s^{-1}. The findings will be of interest to the tidal stream energy industry and

are expected to lead to greater confidence of performance and load predictions for devices in unsteady flow.

The turbulence intensity at 5 m above the seabed was found to be relatively constant over the tidal cycle, at approximately 12–13% in the streamwise direction and 9–10% and 7–8% in the transverse and vertical directions, respectively. A much greater degree of scatter was found within the computed integral time scales and length scales, which averaged 6 s and 11–14 m in the streamwise direction at maximum flow, respectively. The transverse and vertical integral scales were of significantly smaller magnitude.

The velocity spectra, computed at maximum flow, exhibited an integral subrange, and evidence of local isotropy was found between the streamwise and transverse spectral energy. The spectra conformed well to empirical models for atmospheric boundary layer turbulence, implying that a realistic tidal flow could be synthesized using such models. This agreement also appears to suggest that existing analytical models for the rotational sampled spectrum will be useful, in lieu of measurements of the transverse and vertical spatial coherence of the turbulence.

The authors acknowledge ScottishPower Renewables and Andritz Hydro Hammerfest for provision of the dataset used in this study. The assistance from Mr Craig Love of Andritz Hydro Hammerfest and Mr Peter Wilson and Dr Emmanuel Osalusi of Partrac Ltd, Glasgow, UK, is greatly appreciated. The authors also wish to thank Professor J.M.R. Graham of Imperial College, London, UK, for providing valuable guidance. This research has been conducted as part of a PhD programme and I.A.M. wishes to acknowledge the financial support from the Bright Futures Top Achiever Doctoral Scholarship of New Zealand.

References

1. Marsh G. 2009 Wave and tidal power: an emerging new market for composites. *Reinf. Plast.* **53**, 20–24. (doi:10.1016/S0034-3617(09)70220-6)
2. Osalusi E. 2010 Analysis of wave and current data in a tidal energy test site. PhD thesis, Heriot-Watt University, Institute of Petroleum Engineering, Edinburgh, UK.
3. Li Y, Colby JA, Kelley N, Thresher R, Jonkman B, Hughes S. 2010 Inflow measurement in a tidal strait for deploying tidal current turbines: lessons, opportunities and challenges. In *Proc. ASME 2010 29th Int. Conf. on Ocean, Offshore and Arctic Engineering* (*OMAE2010*), *Shanghai, China, 6–11 June 2010*, vol. 3, pp. 569–576. New York, NY: American Society of Mechanical Engineers.
4. Grant HL, Stewart RW, Moilliet A. 1962 Turbulence spectra from a tidal channel. *J. Fluid Mech.* **12**, 241–268. (doi:10.1017/S002211206200018X)
5. Heathershaw AD. 1979 The turbulent structure of the bottom boundary layer in a tidal current. *Geophys. J. Int.* **58**, 395–430. (doi:10.1111/j.1365-246X.1979.tb01032.x)
6. Bowden KF, Fairbairn LA. 1956 Measurements of turbulent fluctuations and Reynolds stresses in a tidal current. *Proc. R. Soc. Lond. A* **237**, 422–438. (doi:10.1098/rspa.1956.0188)
7. Bowden KF. 1962 Measurements of turbulence near the sea bed in a tidal current. *J. Geophys. Res.* **67**, 3181–3186. (doi:10.1029/JZ067i008p03181)
8. Bowden KF, Howe MR 1963 Observations of turbulence in a tidal current. *J. Fluid Mech.* **17**, 271–284. (doi:10.1017/S0022112063001300)
9. Bowden KF, Ferguson SR. 1980 Variations with height of the turbulence in a tidally-induced bottom boundary layer. In *Marine Turbulence: Proc. 11th Int. Liège Colloquium on Ocean Hydrodynamics* (ed. JCJ Nihoul), pp. 259–286. Elsevier Oceanography Series, vol. 28. Amsterdam, The Netherlands: Elsevier.
10. Voulgaris G, Trowbridge JH. 1998 Evaluation of the acoustic Doppler velocimeter (ADV) for turbulence measurements. *J. Atmos. Oceanic Technol.* **15**, 272–289. (doi:10.1175/1520-0426(1998)015<0272:EOTADV>2.0.CO;2)
11. Chanson H, Trevethan M, Aoki A. 2008 Acoustic Doppler velocimetry (ADV) in small estuary: field experience and signal post-processing. *Flow Meas. Instrum.* **19**, 307–313 (doi:10.1016/j.flowmeasinst.2008.03.003)
12. Goring DG, Nikora VI. 2002 Despiking acoustic Doppler velocimeter data. *J. Hydraul. Eng.* **128**, 117–126. (doi:10.1061/(ASCE)0733-9429(2002)128:1(117))
13. Thomson J, Polagye B, Richmond M, Durgesh V. 2010 Quantifying turbulence for tidal power applications. In *Proc. OCEANS 2010*, *Seattle, WA, 20–23 September 2010*. New York, NY: IEEE.

14. Rusello PJ. 2009 A practical primer for pulse coherent instruments. Nortek technical note TN-027. NortekUSA, USA.
15. Bendat JS, Piersol AG. 1971 *Random data: analysis and measurement procedures*. New York, NY: Wiley-Interscience.
16. Trevethan M. 2007 A fundamental study of turbulence and turbulent mixing in a small subtropical estuary. PhD thesis, University of Queensland, Australia.
17. Milne IA, Sharma RN, Flay RGJ, Bickerton S. 2010 The role of onset turbulence on tidal turbine blade loads. In *Proc. 17th Australasian Fluid Mechanics Conf., Auckland, New Zealand, 5–9 December 2010* (eds GD Mallinson, JE Cater). Auckland, New Zealand: Faculty of Engineering in association with the Centre for Continuing Education, The University of Auckland.
18. Stacey MT, Monismith SG, Burau JR. 1999 Measurements of Reynolds stress profiles in unstratified tidal flow. *J. Geophys. Res.* **104**, 10 933–10 949. (doi:10.1029/1998JC900095)
19. Nezu I, Nakagawa H. 1993 *Turbulence in open-channel flows*. Rotterdam, The Netherlands: A. A. Balkema.
20. Cook NJ. 1985 *The designer's guide to wind loading of building structures. I. Background, damage survey, wind data, and structural classification*. London, UK: Butterworths.
21. Engineering Sciences Data Unit. 1985 *Characteristics of atmospheric turbulence near the ground. Part 2. Single point data for strong winds (neutral atmosphere)*. Item no. 85020. London, UK: ESDU.
22. Lien R-C, Sanford TB. 2000 Spectral characteristics of velocity and vorticity fluxes in an unstratified turbulent boundary layer. *J. Geophys. Res.* **105**, 8659–8672. (doi:10.1029/2000JC900031)
23. Connell JR. 1982 The spectrum of wind speed fluctuations encountered by a rotating blade of a wind energy conversion system. *Solar Energy* **29**, 363–375. (doi:10.1016/0038-092X(82)90072-X)